Stochastic Dynamic Approach to Transport Phenomena

Manuel Laso
Institut für Polymere, Eidgenössische Technische Hochschule, ETH-Zentrum, CH-8092 Switzerland

A stochastic dynamic approach to the equations of change is introduced here, which first is applied to linear equations and is based on the formal analogy between certain forms of the equations of change and the Fokker-Planck equation. A stochastic differential equation associated with the Fokker-Planck equation can be derived from the latter and solved numerically, thus yielding the solution to the original equation of change. The proper treatment of boundary conditions is essential for the success of the method. We show that the method is able to handle the eight fundamental types of boundary conditions (Carslaw and Jaeger, 1959; Crank, 1975). In addition, the stochastic dynamic approach provides a deeper insight in the physical processes underlying transport phenomena than do traditional techniques.

Introduction

Since the appearance of Bird, Stewart, and Lightfoot's *Transport Phenomena* (Bird et al., 1960) the field of transport phenomena has been recognized as a distinct engineering subject and is nowadays considered one of the key engineering sciences. The basic laws of mass, momentum, and energy transport constitute the general framework within which the overwhelming majority of chemical engineering problems are formulated. The partial differential equations known as *equations of change* determine how mass, momentum, and energy change with position and time within a region of space.

Traditionally, the equations of change have been solved either analytically or numerically by means of time-space discretization techniques such as finite differences and finite elements. Analytical solutions are known for only a relatively reduced but important class of problems (Bird et al., 1987a; Carslaw and Jaeger, 1959; Crank, 1975; Landau and Lifshitz, 1987). More demanding problems often require numerical methods based on discretization. Their versatility and power combined with the availability of increasingly powerful hardware have made numerical techniques the method of choice for complex problems and geometries (Chawla, 1989; Hirata and Kasagi, 1988; Markatos, 1986; Patankar, 1980).

The purpose of this article is to introduce a novel approach to the solution of the equations of change. Generally, these equations contain, among others, convective and diffusive terms. These terms can be made to correspond formally with the drift and diffusion terms of the Fokker-Planck equation (FPE). The FPE is itself a partial differential equation (Risken, 1989) like the original equation of change, and therefore not easier to solve. The advantage of the formal analogy between the equation of change and the FPE is that the latter can be cast in the form of a stochastic differential equation (SDE). This SDE is much easier to solve numerically than the FPE; indeed, it can be solved with straightforward techniques which are flexible and far simpler to implement than standard discretization schemes like finite differences, finite elements, or finite volumes. The analogy between the equation of change of the FPE guarantees that the solution of the associated SDE yields the solution of the original equation of change. While mapping the original equation of change onto an SDE is easy, the treatment of boundary conditions turns out to be a more critical and interesting task.

Similar stochastic methods have been very successfully exploited in the context of kinetic theory of polymer systems (Ermak and McCammon, 1978; Fixman, 1986; Öttinger, 1989, 1990) but, to our knowledge, have not been applied to the macroscopic equations of change.

In this article, we introduce the fundamental ideas of the stochastic dynamic method. The main emphasis of the article is on the development of techniques for the treatment of boundary conditions. General algorithms are developed for the eight fundamental boundary conditions described in Carslaw and Jaeger (1959) and Crank (1975). It is further shown that the stochastic approach provides a natural microscopic interpretation of the processes underlying the continuum-mechanical equations of change.

Fokker-Planck Equation

A Fokker-Planck equation was first used by Fokker and Planck to study Brownian motion in a radiation field (Risken, 1989). The FPE is also known as Kolmogorov's forward equation in the theory of Markov processes in mathematically oriented works, as Klein-Kramers equation, as Smoluchowski equation, or as diffusion equation in polymer kinetic theory (Bird et al., 1987b). The FPE can be written in the general form:

$$\frac{\partial}{\partial t}p(t,x)=-\frac{\partial}{\partial x}\cdot[A(t,x)p(t,x)]+\frac{1}{2}\frac{\partial}{\partial x}\frac{\partial}{\partial x}:[D(t,x)p(t,x)] \tag{1}$$

where t stands for time, x is a d-dimensional vector of coordinates (not necessarily Cartesian), $p(t, x)$ is a probability density, $A(t, x)$ is a d-dimensional vector, and $D(t, x)$ is a positive-semidefinite symmetric $d\times d$ matrix. The term containing A is called the drift term and the term containing D, the diffusion term. The FPE is a parabolic linear partial differential equation that arises in the description of a macroscopic system in which some microscopic degrees of freedom are treated in a stochastic fashion, thus leading to macroscopic variables that fluctuate in a stochastic way. It is the equation of motion for the distribution function of fluctuating macroscopic variables and it governs the time evolution of the probability density $p(t, x)$ for a given system. The FPE has been widely used in many different contexts and it is ubiquitous in kinetic theory. For further details, the reader is referred to the monographs of Gardiner (1983), Honerkamp (1990), van Kampen (1981), Öttinger (1994), and Risken (1989).

The form of the FPE is quite general, since the components of both A and D can be functions of time and of the coordinates x. An inspection of the FPE suggests the possibility of formally writing a wide class of transport equations as FPEs. The vector $A(t, x)$ and the matrix $D(t, x)$ are determined by identifying the corresponding terms in the partial differential equation to be solved. For example, the heat conduction equation in an anisotropic homogeneous two-dimensional solid domain Ω, is:

$$\rho c\frac{\partial T}{\partial t}=K_{11}\frac{\partial^2 T}{\partial x_1^2}+K_{22}\frac{\partial^2 T}{\partial x_2^2}+(K_{12}+K_{21})\frac{\partial^2 T}{\partial x_1\partial x_2}$$

which has the form of a FPE, if we make the identifications:

$$x\mapsto\begin{bmatrix}x_1\\x_2\end{bmatrix}\qquad p(t,x)\mapsto T(t,x)\qquad A(t,x)\mapsto\begin{bmatrix}0\\0\end{bmatrix}$$

$$D(t,x)\mapsto\begin{bmatrix}\frac{K_{11}}{\rho c}&\frac{K_{12}}{\rho c}\\\frac{K_{21}}{\rho c}&\frac{K_{22}}{\rho c}\end{bmatrix}$$

Assuming we can solve the FPE, the next step is to obtain the temperature (or concentration) field from the probability density $p(t, x)$. This requires a (trivial) rescaling because the integral of $p(t, x)$ over the x-space has to be unity. Besides, in heat-transfer problems the conserved quantity is energy, that is, $p(t, x)$ must be identified with the energy content and then converted into a temperature using the specific heat and the density. In general, it can be said that partial differential equations that express a conservation law have good chances of being successfully treated with the stochastic dynamic approach.

In many transport problems the boundary conditions correspond to a net flux of heat (or mass, or momentum) through the boundaries of the integration domain, that is, the quantity of interest is not conserved over the integration domain. However, we are free to define the probability density $p(t, x)$ in the integration domain Ω supplemented by an additional domain Ω^*. The integral of $p(t, x)$ over $\Omega\cup\Omega^*$ will then be normalized to one, but the integral over Ω need not be so normalized. The introduction of Ω^* is unproblematic, and we do not need to define it explicitly. Its meaning is that of a reservoir (sink or source) of probability from which we can take or to which we can give back probability in order to fulfill the boundary conditions. We consider it, to use van Kampen's term (van Kampen, 1981, p. 161), a *limbo* domain which needs not be explicitly considered and whose role is that of a probability reservoir. In case of no flux of heat (or mass, or momentum) in or out of the domain Ω, Ω^* is not required. The energy in the integration domain will be automatically conserved by the conservation of probability. If there is net flux, the integral of $p(t, x)$ in Ω will change with time, but the conversion between probability, energy (or mass, or momentum), and temperature (or concentration, or velocity) will always be possible through a boundary condition or some other physical requirement, as will be shown below.

An obvious restriction to the use of the FPE analogy is that the FPE is a linear equation. A and D may depend on t and x, but not on $p(t, x)$ itself. Nonlinear equations can be treated within the more general formalism of master equation/jump processes (Gardiner, 1983; Honerkamp, 1990; van Kampen, 1980). This article concentrates on the linear case.

Once the equation of change has been written as a FPE, we are still confronted with a partial differential equation of comparable complexity. Although analytical methods of solution exist (Risken, 1989; Gardiner, 1983) they can be applied to quite specific problems only and are not essentially different from those used to solve partial differential equations in chemical engineering. Here we follow an alternate and very general way based on an associated stochastic differential equation (SDE).

Stochastic Differential Equation

Assuming A and D satisfy certain conditions (Lipschitz, linear growth, continuity, symmetric positive semi-definite D), it can be proved (Kallianpur, 1980) that the FPE (Eq. 1) corresponds to a Markov process with the following infinitesimal generator:

$$\mathcal{L}_t=A(t,x)\cdot\frac{\partial}{\partial x}+\frac{1}{2}D(t,x):\frac{\partial}{\partial x}\frac{\partial}{\partial x}$$

and the Markov process is the solution of the multivariate stochastic differential equation:

$$dX_t=A(t,X_t)dt+B(t,X_t)\cdot dW_t \tag{2}$$

where $A(t, x)$ is the same as in Eq. 1 and:

$$D(t, x) = B(t, x) \cdot B^T(t, x) \tag{3}$$

In other words, the SDE (Eq. 2) is the stochastic counterpart of the deterministic FPE (Eq. 1); the transition probabilities for the solution of the SDE are governed by the FPE and vice-versa: if we are given the FPE, we can construct an associated SDE. Stochastic differential equations have a rigorous mathematical background (Itô, 1942; Gard, 1988; Kloeden and Platen, 1992). They differ from deterministic ODEs in the term containing the differential of the Wiener process W. The Wiener process is a Gaussian process whose increments for disjoint time intervals are uncorrelated Gaussian random variables with:

$$\langle W_t - W_{t'} \rangle = 0 \quad \langle (W_t - W_{t'})^2 \rangle = |t - t'|$$

that is, the mean-square increment of the Wiener process grows linearly in time. In practice W is a d-dimensional vector of independent Gaussian variables.

Although stochastic differential equations have not generally been recognized as the common source of all the phenomena usually described by FPEs, it is much more intuitive to work directly with stochastic processes rather than with deterministic auxiliary equations for probability distributions. In particular, one can easily obtain computer simulation algorithms by developing numerical integration procedures for SDEs (Öttinger, 1993). Herein lies the main advantage of going from the FPE to the associated SDE: the SDE (Eq. 2) has a much simpler form than Eq. 1 and the numerical integration of the SDE is far simpler than the integration of the FPE. The probability distribution $p(t, x)$, or, after conversion, the temperature or concentration field, is obtained by averaging over an ensemble of many *sample paths* or *trajectories*. In the context of the SDE, the limbo domain Ω^* (discussed above in connection with the conservation of probability) is a reservoir of sample paths. The conservation of the total $p(t, x)$ over $\Omega \cup \Omega^*$ corresponds to the conservation of the total number of trajectories in the ensemble. In the case of nonzero flux, the nonconservation of $p(t, x)$ over Ω means that new trajectories are started or terminated in order to impose a boundary condition.

The decomposition of the diffusion matrix D according to Eq. 3 (Choleski decomposition) is always possible due to its positive semi-definiteness, but, in general, not unique (D contains $d(d+1)/2$ independent elements, whereas B contains d^2). For different choices of B, the sample paths will be different; however, the probability distribution function $p(t, x)$, all transition probabilities, and hence all averages will be identical. This is all one is interested in when working with the FPE.

Example

In order to illustrate the method, let us consider the time-dependent heat conduction equation in a one-dimensional homogenous solid:

$$\frac{\partial T}{\partial t} = \alpha \frac{\partial^2 T}{\partial x^2} \tag{4}$$

where T is the temperature, t is time, x the spatial coordinate, and α is the thermal diffusivity. Equation 4 has the form of a one-dimensional FPE with $A(t, x) = 0$ and $D(t, x) = 2\alpha$. Its associated SDE, according to Eq. 2, is:

$$dX_t = \sqrt{2\alpha}\, dW_t \tag{5}$$

where W is a one-dimensional Wiener process (Gardiner, 1983; Honerkamp, 1990; Öttinger, 1993). A remarkable aspect of Eq. 5 is its simplicity compared with Eq. 4. The problem has been reduced from that of solving a *second-order partial differential equation* to that of solving an *ordinary first-order* SDE. This is reminiscent of the reduction in transcendentality achieved, for example, by means of a Laplace transformation. The second striking aspect of Eq. 5 is that the stochastic process counterpart to the deterministic temperature field is a Wiener process, the epitome of a diffusive process. The individual trajectories perform random walks with highly irregular, nowhere differentiable paths. In this example, the transformation between the FPE and the SDE brings to the fore the microscopic aspect of the purely diffusive heat-transfer process, which is lost in the usual mathematical derivation of the equations of change. This physical interpretation, although not necessary for the solution procedure, can be very enlightening when dealing with complex problems (Öttinger, 1989).

Solving the SDE

Kloeden and Platen (1992) provide a comprehensive account of the relatively modern field of numerical solution of SDEs. The most efficient and widely applicable approach to solving SDEs seems to be the simulation of sample paths of time discrete approximations. Here we will work with the simplest integration scheme: the Euler-Maruyama approximation (Maruyama, 1955; Kloeden and Platen, 1992). For a given time discretization of the time interval $[0, t_{end}]$:

$$0 = t_0 < t_1 < \ldots < t_i < \ldots < t_{N_{step}} = t_{end}$$

which we can assume to be equidistant:

$$t_{i+1} = t_i + \Delta t \quad i = 0, \ldots N_{step} - 1$$

the time discrete approximation to the SDE (Eq. 5) is:

$$Y_{i+1} = Y_i + \sqrt{2\alpha \Delta t}\, W_i \quad i = 0, 1, \ldots N_{step} - 1 \tag{6}$$

with initial value $Y_0 = x_0$, which can be a stochastic variable itself. W_i is a Gaussian random number with zero mean and unit variance. Furthermore, the Gaussian numbers for different time steps are independent, in direct correspondence to the independence of the increments for the Wiener process. The expression for a multidimensional SDE (Eq. 2) is only slightly more complex (Kloeden and Platen, 1992; Petersen, 1992). A time-discretized sample path of the SDE (Eq. 5) is trivially produced by repeatedly applying the stochastic difference equation (Eq. 6). In this way, an ensemble of M sample paths can be generated. The probability density, which is the solution of the FPE and, therefore, (after conversion to temperature) the solution to our original problem, is obtained by counting over the sample paths in the ensemble. The probability density at a given time t in any interval $[x, x + \Delta x]$ is proportional to the local density of the ensemble of independent trajectories.

It is obtained by counting how many sample paths are in the interval $[x, x+\Delta x]$ at time t and normalizing.

In the previous description, the generation of sample paths was assumed to be serial in time, the averaging procedure taking place after all the paths had been generated. An equally valid but more intuitive method is to generate many sample paths in parallel, possibly the whole ensemble, and integrate all of them simultaneously. $p(t, x)$ is obtained by gridding the domain of integration in N_{bin} bins and determining how many of the M paths are in each bin at a given time. This grid is just a measuring device and not a part of the simulation; in fact, it does not have to be used at every integration step but only at those times for which we want to know $T(t, x)$. Additionally, if we are not interested in the whole $T(t, x)$ field, but only in the values at certain locations, it is enough to place "measuring" bins at those locations and nowhere else. After proper normalization and conversion from energy units into temperature units, the resulting histogram is the desired temperature field (with the proviso that the value we obtain for a bin corresponds to the integral average of $p(t, x)$ over that bin). Better temporal and spatial resolution can be obtained by reducing the step size and increasing the number of sample paths.

It is important to emphasize that in all cases we are only interested in a weak solution of the SDE, that is, a solution that leads to the same $p(t, x)$ and to the same averages. The approximating process Y is said to converge in the weak sense with order β if for any polynomial $g(\ )$, there exist a constant K and a positive constant δ_0 such that:

$$|E[g(X_{t_{\text{end}}})] - E[g(Y_{N\text{step}})]| \leq K\Delta t^{\beta}$$

for any discretization with maximum time step $\Delta t \in (0, \delta_0)$. In the deterministic case D is identically zero and this criterion reduces to the usual deterministic criterion if we take $g(x) = x$.

Initial and Boundary Conditions

Up to now no mention has been made of initial conditions (ICs) and boundary conditions (BCs). The transformation rule between FPE and SDE concerns only the dynamics of the stochastic process to be simulated, independent of initial and boundary conditions. In our example, the SDE to be integrated is the same for all boundary conditions, namely Eq. 5. This is indeed what we should expect: heat conduction occurs due to diffusion. The boundary conditions *cannot* modify this behavior. They will certainly affect the fate of the energy flowing in our integration domain, that is, the fate of the individual sample paths, whether they are absorbed, reflected, and so on, but not the diffusive mechanism of transport.

While the transformation between the FPE (Eq. 1) and the SDE (Eq. 2) can be done by applying a simple *recipe*, there is no equivalently obvious rule for the treatment of the BCs. The treatment of boundary conditions can be in fact the most demanding part of such a stochastic simulation (Öttinger, 1989). Next, we will develop general algorithms to treat all important boundary conditions that occur in practice. We study the eight fundamental types of boundary conditions as they appear in Crank's enumeration (Crank, 1975, pp. 8–10) and apply them to our one-dimensional heat-transfer problem. For each one of them, a numerical example is solved in order to verify the correctness of the algorithms. For simplicity reasons, we will assume in the numerical examples all physical properties (like conductivity, specific heat, latent heat, density, and so on) to be equal to 1 and all temperatures to be normalized between 0 and 1. For the determination of the temperature profile, we use a histogram of N_{bin} bins of equal width $\Delta x = 1/N_{\text{bin}}$. Analytical solutions to the numerical examples are taken from Carslaw and Jaeger (1959) and Crank (1975).

Case A: prescribed temperature at the boundary: $T = T_b$ at $x = x_b$

In the context of the Stochastic Dynamic method, the condition $T = T_b$ at $x = x_b$ implies that the density of trajectories in the region outside Ω immediately adjacent to the boundary (which we will call the *boundary region*) has to be kept constant during the whole integration. If, for example, the integration domain extends from $x_b = 0$ towards $+\infty$, we take $[x_b - \Delta x_b, x_b]$ as the boundary region. The BC is enforced by starting as many new trajectories as necessary at every time step in the boundary region to compensate for the ones that have left it and entered the integration domain Ω. Since the increments in Eq. 6 are typically of $O((\alpha\Delta t)^{1/2})$, it is enough to take the width of the boundary region Δx_b large with respect to $(\alpha\Delta t)^{1/2}$. Let's assign N_b to the number of trajectories in the boundary region that we want to correspond to $T = T_b$; let c_b and ρ_b be the specific heat and the density of the boundary region respectively. The values of c_b, ρ_b, Δx_b, and N_b can be chosen arbitrarily; the higher the value of N_b, the lower the statistical noise in the result. Once these values have been chosen, the temperature in a bin $[x, x+\Delta x]$ within the integration domain, at a given time t, is obtained by counting the number of trajectories that are present in that bin at t and multiplying by the normalization factor:

$$NF_{(a)} \equiv \frac{\Delta x_b \rho_b c_b T_b}{N_b \Delta x \bar{\rho}(t, x)\bar{c}(t, x)}$$

where the overbar denotes an integral average value over the interval $[x, x+\Delta x]$ at time t (assuming space- and time-dependent physical properties). The factor $NF_{(a)}$ is obtained by converting a number of trajectories, that is, an energy into a temperature (whence the presence of the specific heat), both for a given bin and for the boundary region. $NF_{(a)}$ is then obtained from the equality of the two $N\Delta x\rho cT$ expressions.

The size of the measuring bin Δx can be chosen freely and independently of $\alpha\Delta t$, so long as the diffusive behavior of the trajectories at the coarse-grained level of Δx is preserved, that is, so long as $\alpha\Delta t \ll \Delta x^2$. In the numerical example below we will illustrate what are the consequences of violating this condition.

The initial value x_0 for the N_b sample paths in the boundary region is itself a random variable uniformly distributed in $[x_b - \Delta x_b, x_b]$. At every integration step, some trajectories will leave the boundary region and enter the integration domain Ω where they will be further integrated and where they will make a contribution to the temperature of the bin in which they are located at every time step. In order to compensate for the trajectories that diffuse from the boundary region into Ω, the boundary region has to be refilled uniformly with new trajectories at every integration step. The temperature field in Ω at any time is obtained by counting the number of trajectories

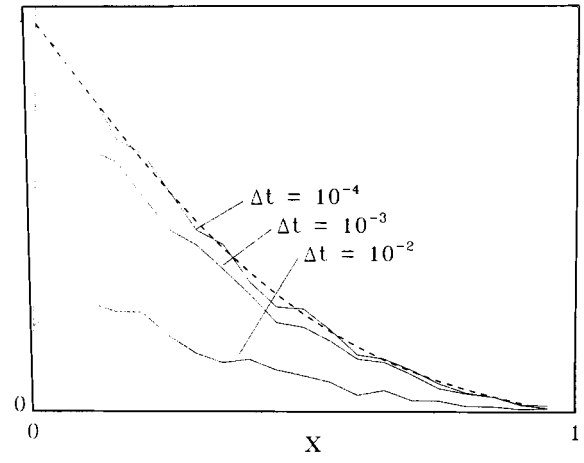

Figure 1. Boundary conditions a: prescribed temperatures at the boundaries.

Comparison of analytical (- - - -) and computed (—) temperature profiles at $t=0.1$ for different integration time steps. $N_{bin}=20$, $N_b=1{,}000$, $\Delta x_b=0.05$, $c_b=\rho_b=c_b=1$.

in each bin of width Δx and normalizing with $NF_{(a)}$. Although the total number of trajectories in Ω increases during the integration, the normalization poses no difficulties whatever.

This BC is especially easy to implement when $T_b=0$. In the stochastic approach this is realized by an *absorbing boundary* (Gardiner, 1983; Risken, 1989): zero temperature in the boundary region implies that all trajectories that reach the absorbing boundary are simply terminated, that is, they leave Ω and cease to contribute to the temperature field in the integration domain. The BC $T=T_b=0$ is obviously simpler to implement than $T=T_b\neq 0$ and, although it seems to be a rather special case, it is in practice very useful: an alternate way of handling boundaries of prescribed nonzero temperature is to make a transformation of variables such that the transformed field has a value of zero at the boundaries.

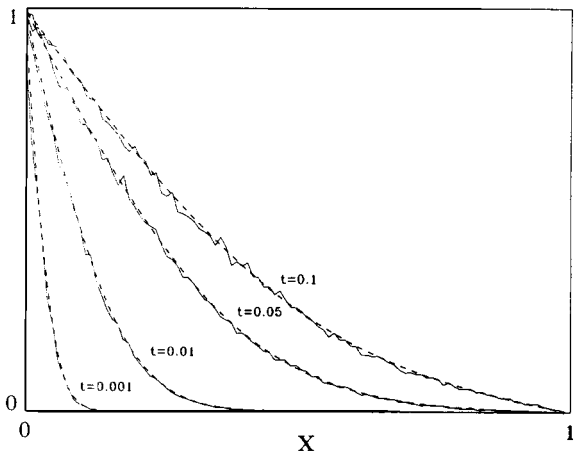

Figure 2. Boundary conditions a: temperature profiles at different times.

Comparison of analytical (- - - -) and computed (—) $N_{bin}=100$, $N_b=5{,}000$, $\Delta t=10^{-5}$; other parameters are the same as for Figure 1.

Example:
Integration domain: [0, 1]
Boundary conditions: $T=1$ at $x=0$, $T=0$ at $x=1$, for $t>0$
Initial conditions: $T=0$ for $0\leq x\leq 1$
Analytical solution:

$$T^{an}(x,t)=(1-x)-\frac{2}{\pi}\sum_{k=1}^{\infty}\frac{1}{k}e^{-k^2\pi^2 t}\sin k\pi x$$

The procedure described above was applied to the heat conduction equation in the interval [0, 1] with temperature prescribed at both boundaries, one of them being $T_b=0$. Figure 1 represents the analytical (dashed) together with the computed temperature profiles (solid) at $t=0.1$, the latter obtained with different integration time steps, for fixed number of bins N_{bin} ($N_{bin}=20$) and of trajectories in the boundary region N_b ($N_b=10^3$). When comparing the analytical and the stochastic solutions we have to keep in mind that the Stochastic Dynamic method yields the value of:

$$\frac{1}{\Delta x}\int_x^{x+\Delta x}T^{an}(z,t)dz \qquad (7)$$

that is, the integral average over each interval. In Figure 1 and in all subsequent plots, the analytical solution shown has been calculated using Eq. 7 for $x=0$, Δx, $2\Delta x$, ..., $(N_{bin}-1)\Delta x$, which, unless the curvature of $T^{an}(x,t)$ is large, will be almost identical to $T_{an}(\Delta x/2)$, $T^{an}(3\Delta x/2)$, and so on. As mentioned before, when the time step is too large, $\Delta t=10^{-2}$ and $\Delta t=10^{-3}$ in Figure 1, the stochastic solution is qualitatively wrong. According to Eq. 6 the increment per time step is of $O[(\alpha\Delta t)^{1/2}]$. If this is larger than $O(\Delta x)$, the trajectory typically jumps over more than one bin per time step and the diffusive behavior is lost at the coarse-grained level defined by Δx. This bound is analogous to the quadratic relationship between time step and spatial discretization in standard finite element or finite difference techniques due to stability requirements of the resulting algebraic system.

Once the time step fulfills $\alpha\Delta t\ll\Delta x^2$ (curve for $\Delta t=10^{-4}$ in Figure 1), the stochastic solution is in perfect agreement with the analytical one. It is important to emphasize once more that this is the only way in which the time step Δt and the bin size Δx are related. The bins are just a measuring device, and not a part of the simulation; Δx must never appear in the dynamics of the trajectories and Δx can be chosen arbitrarily so long as $\Delta x^2\gg\alpha\Delta t$ is satisfied.

Figure 2 shows the temperature field at four different times using $\Delta t=10^{-5}$. Within statistical uncertainty, agreement is perfect. An interesting feature of the stochastic approach is the absence of oscillations at short times in the computed temperature field caused by the singularity at $t=0$, $x=0$. When using traditional finite elements or finite difference methods, it is necessary to develop analytical expansions applicable for small times or to transform the variables so that the singularity is removed (Crank, 1975). Otherwise, spurious oscillations appear. This behavior is unphysical and of purely mathematical origin. In the stochastic method however, the singularity at $t=0$ is harmless: the diffusive behavior of the trajectories will always ensure a smooth profile no matter how close to the singularity.

As the problem has been formulated, we have a boundary at which trajectories are terminated (heat sink) and another where new trajectories are fed into the system (heat source). The new trajectories perform a random walk in the domain and presently leave it. This corresponds exactly to the physical picture of diffusive heat transfer from one boundary to the other. However, it is possible to cast the problem in a slightly different way in which only absorbing boundaries appear. If we use the ansatz:

$$\bar{T} = 1 - x - T$$

$\bar{T}$ satisfies the same PDE as T with the advantage that now both boundaries are absorbing. In general, the new field will satisfy a different PDE and therefore lead to a different SDE, but after undoing the transformation, the resulting $p(t, x)$ will be identical.

Case B: prescribed heat flux: $-k\partial T/\partial x = F_b$ at $x = x_b$

Since this BC involves a derivative of the temperature field and the stochastic solution is inherently *noisy*, one could expect difficulties for the stochastic approach. This is however not the case, because, although formulated as a derivative, this BC has the physical meaning of a flux. This flux can be naturally incorporated in the stochastic simulation as a probability current so that derivatives need never be computed. The way to implement this type of BC is to start a fixed, but otherwise arbitrarily chosen, number N_{Flux} of trajectories per integration step in the bin that is immediately adjacent to the boundary but within Ω (which we will call the *boundary bin*), irrespective of how many trajectories are already present in it. In the course of the integration, these trajectories will subsequently diffuse throughout the integration domain and contribute to the temperature field. Trajectories that attempt to leave Ω through the boundary at which the flux is imposed are reflected back into Ω as will be explained in the next section (see boundary condition c) below. The temperature in a given bin $[x, x+\Delta x]$ is obtained by multiplying the instantaneous number of trajectories in that bin by the conversion factor:

$$NF_{(b)} \equiv \frac{\Delta t}{N_{\text{Flux}} \Delta x \bar{\rho}(t, x) \bar{c}(t, x)}$$

The algorithm is completed by specifying the location x_0 (within the boundary bin) at which the N_{flux} trajectories should be started at every time step. Whereas we can start our N_{flux} trajectories only at $t = 0$, Δt, $2\Delta t$, and so on, in reality, heat flows continuously into the integration domain. If we could somehow start new trajectories at $x_0 = x_b$ *continuously* between two integration steps, these trajectories would diffuse a typical length of $O((\alpha \Delta t)^{1/2})$ during the step Δt (and the resulting local temperature field would be a convolution of a step function with a Gaussian). If our discrete integration process is to approximate the continuous process, the new trajectories must not be started at $x_0 = x_b$ (which would correspond to a delta function at $x = x_b$) but rather at a location x_0 such that $|x_0 - x_b| = O((\alpha \Delta t)^{1/2})$. In this way we account for the characteristic broadening of the distribution of the N_{Flux} new trajectories during a time step. Although the exact value of x_0 is not very important as long as its order of magnitude is correct, failure to account for this effect severely reduces the convergence properties of the algorithm.

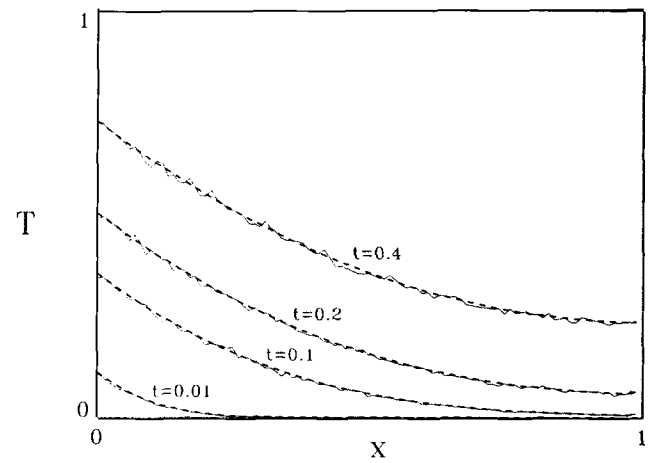

Figure 3. Boundary conditions b: prescribed heat flux.

Comparison of analytical (- - - -) and computed (—) temperature profiles at four different times. $N_{\text{bin}} = 100$, $N_{\text{Flux}} = 10$, $\Delta t = 10^{-5}$.

Example:

Integration domain: [0, 2]

Boundary conditions: $\partial T/\partial x = -1$ at $x = 0$, $\partial T/\partial x = 1$ at $x = 2$, for $t > 0$

Initial conditions: $T = 0$ for $0 \le x \le 2$

Analytical solution:

$$T^{\text{an}}(x, t) = t + \frac{3(1-x)^2 - 1}{6} - \frac{2}{\pi^2} \sum_{k=1}^{\infty} \frac{(-1)^k}{k^2} e^{-k^2 \pi^2 t} \cos k\pi (1-x)$$

This example corresponds to the constant influx of heat from both sides of the integration domain $\Omega = \{[0, 2]\}$. In Figure 3 the left half of the analytical temperature profile (symmetry about $x = 1$) is depicted at four different times together with the solutions obtained with the stochastic method. We see that a BC involving a derivative can be successfully handled in the stochastic approach. In the results presented in Figure 3, the N_{Flux} new trajectories per integration step were started at $x_0 = (\alpha \Delta t)^{1/2}$.

Case C: heat insulated boundary: $\partial T/\partial x = 0$ at $x = x_b$

The BC for an insulated boundary is expressed mathematically as a vanishing temperature gradient at the boundary. In the stochastic simulation we directly apply the physical interpretation of the BC, namely zero flux through the boundary. This corresponds to a *reflecting boundary* (Gardiner, 1983; Risken, 1989). When a trajectory attempts to go beyond the boundary, it is reflected back into the domain and the time integration continued: assuming the trajectory to be at $Y_i < x_b$ (within Ω) at $t = t_i$ and at $Y_{i+1} > x_b$ (outside Ω) at $t = t_{i+1}$, the reflection is implemented by changing the latter value to $Y_{i+1} = x_b - |x_{i+1} - x_b|$. This procedure is accurate to all orders of Δt, thanks to the reflection property of the Wiener process.

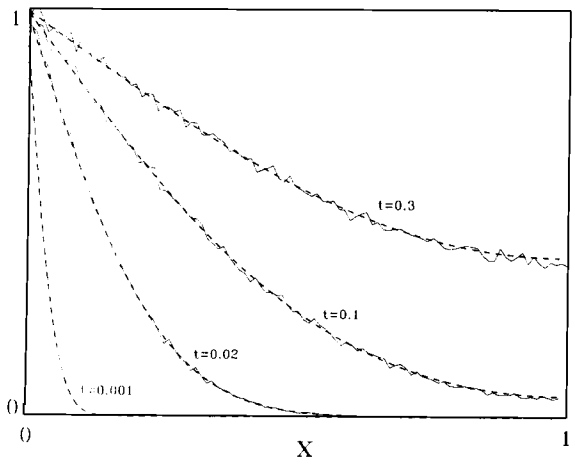

Figure 4. Boundary conditions c: insulated boundary.

Comparison of analytical (- - - -) and computed (—) temperature profiles at four different times. $N_{bin}=100$, $N_b=4{,}500$, $\Delta t=10^{-5}$.

Example:
Integration domain: [0, 1]
Boundary conditions: $T=1$ at $x=0$, $\partial T/\partial x=0$ at $x=1$ for $t>0$
Initial conditions: $T=0$ for $0\le x\le 1$
Analytical solution:

$$T^{an}(x,\,t)=1+\frac{2}{\pi}\sum_{k=1}^{\infty}e^{-k^2\pi^2 t/4}\sin\frac{k\pi x}{2}\,\frac{\cos k\pi-1}{k}$$

One of the BCs, namely prescribed temperature at $x=0$, has already been discussed earlier in case A. The insulated boundary was implemented according to the algorithm described above. The temperature profiles produced by the stochastic method in Figure 4 are in excellent agreement with the analytical solution. At $t=0.001$ the analytical and stochastic solutions are indistinguishable. Again, no difficulties with the singularity at $t=0$, $x=0$ arise.

The insulated or reflecting boundary is useful in the treatment of problems with symmetry: the stochastic simulation for case B above was actually performed on one half of the total interval. The axis of symmetry at $x=1$ was realized by reflecting back into [0, 1] any trajectory that attempted to go beyond $x=1$.

Case D: "radiation" boundary condition: $-k\partial T/\partial x+h(T_b-T_0)=0$ *at* $x=0$

In heat flow and in spite of its name, the *radiation* BC usually means that the heat flux across the boundary is proportional to the difference between the temperature at the boundary T_b and the temperature of the surrounding medium T_0. Although this BC involves a gradient, its physical interpretation is that of a flux and can therefore be treated as in case B above.

There are two differences with respect to case B: (i) the flux is now variable in time; (ii) its instantaneous value depends on the temperature difference between the boundary and the surroundings and is therefore not known in advance. (i) presents no problems because the method expounded in B holds equally well for time-dependent flux where the number of trajectories to be removed per unit time is variable. We implement (ii) in the stochastic approach by first "measuring" the temperature of the boundary T_b at every time step: we count how many trajectories are currently in the boundary bin $[x_b,\, x_b+\Delta x]$ and normalize this number to a temperature as in case A. Once T_b is known, the heat flux induced by the difference between T_b and T_0 is converted into the number of trajectories to be started in or removed from the boundary bin (depending on the sign of T_b-T_0), just as we did in case B. If trajectories have to be started (positive flux into Ω) we proceed as in case B. If trajectories have to be removed, the naive approach would be to terminate trajectories from the boundary bin. However, the efficient method is to start *negative* or *cold* trajectories that represent outflow of heat from it. In practice this is done in exactly the same way as in cases A, B, or C. We start new *negative* trajectories and propagate them in time in the same way as the *positive* trajectories we have dealt with up to now. Similarly, when starting new negative trajectories the same prescription concerning x_0 as explained in case B has to be followed. The adjective *negative* comes from the fact that they make a negative contribution to the temperature field: the density of negative trajectories is determined in the same manner as for positive ones and the resulting value represents a negative contribution to the temperature field. The use of *negative* trajectories is both intuitively clear and rigorous: *negative* trajectories correspond to a transformation of T which changes its sign, typically of the form $\overline{T}=f(x)-T$, where $f(x)$ is a linear function of x. The underlying dynamics of the individual trajectories are unchanged (*negative* heat diffuses according to the same mechanism as *positive* heat). The following example illustrates this algorithm:

Example:
Integration domain: [0, 1]
Boundary conditions: $-\partial T/\partial x+T_s-T_0=0$ at $x=0$ for $t>0$; $T_0=0.5$
$\partial T/\partial x=0$ at $x=1$, for $t>0$
Initial conditions: $T=1$ for $0\le x\le 1$
Analytical solution:

$$T^{an}(x,\,t)=\frac{1}{2}+\sum_{k=1}^{\infty}e^{-q_k^2 t}\,\frac{\cos[q_k(1-x)]}{(q_k^2+2)\cos q_k}$$

where q_k is the kth solution of:

$$\tan q=\frac{1}{q}\qquad q>0$$

The initial condition $T(t=0)=1$, for $0\le x\le 1$, implies that at $t=0$ the interval [0, 1] should be uniformly filled with a large number of trajectories, namely $N_{bin}\times N_1$, where N_1 is the number of trajectories per bin which we arbitrarily choose to correspond to $T=1$. Unlike in cases A through C, where Ω was empty at the beginning of the integration, now the full ensemble of trajectories is in Ω; Ω^* is empty. However, if we make the transformation $\overline{T}=1-T$, the heat conduction equation and the second BC (reflecting boundary like in case C above) remain unchanged while the term $\partial T/\partial x$ in the first BC changes its sign and $\overline{T}_s=1-T_s$. The initial condition is $\overline{T}=0$

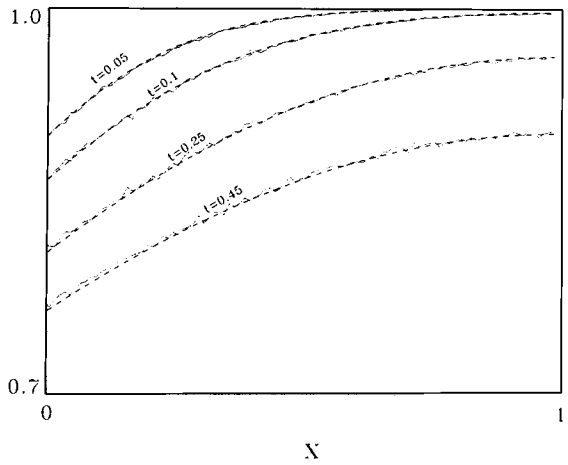

Figure 5. Boundary conditions d: "radiation" boundary conditions.

Comparison of analytical (- - - -) and computed (—) temperature profiles at four different times. Temperature of the surrounding medium $T_0 = 0.5$, $N_{bin} = 100$, $\Delta t = 10^{-5}$, a temperature of 1 corresponds to 4×10^4 trajectories per bin of width Δx.

for $0 \le x \le 1$ (meaning that at the beginning of the simulation Ω is empty) and the flux is now *into* the interval.

The agreement between the analytical solution and the stochastic solution is displayed in Figure 5. The integration of the original equation for T leads to the same results but requires about 70 times more CPU time.

Case E: perfect conductor at the boundary: $-k\partial T/\partial x = \rho_{PC} c_{PC} V_{PC} \partial T_{PC}/\partial t$ at $x = x_b$

The perfect conductor corresponds to a reservoir of energy that has a time-dependent but spatially constant temperature throughout its volume (in mass-transfer problems it would correspond to a perfectly mixed fluid). Heat flows between the reservoir and the domain.

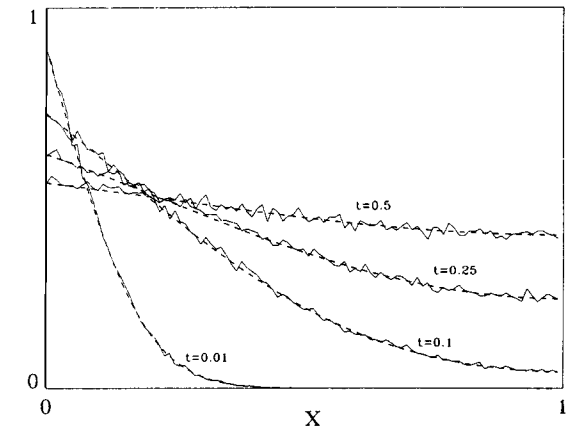

Figure 6. Boundary conditions e: perfect conductor at the boundary.

Comparison of analytical (- - - -) and computed (—) temperature profiles at four different times. The perfect conductor has the same size and physical properties as the integration domain. $N_{bin} = 100$, $\Delta t = 10^{-5}$, a temperature of 1 corresponds to 4×10^3 trajectories per bin.

The stochastic dynamic algorithm is as follows: since the system formed by the integration domain plus reservoir is adiabatic, we identify Ω^* with the reservoir. Trajectories that are originally in Ω^* diffuse into Ω as time advances. Let N_{PC} be the (arbitrarily chosen) number of trajectories that correspond to a temperature of T_{PC}, and V_{PC}, ρ_{PC}, and c_{PC} the volume, density, and specific heat of the reservoir, respectively. In order to implement the transfer from the reservoir into the integration domain, we make use of the condition that the temperature of the boundary is always equal to the temperature of the perfect conductor. The temperature of the perfect conductor at a given time t is given by the ratio of the number of trajectories present in it at t to N_{PC}.

The trajectories in the reservoir *never have to be integrated* since only their number is important, and not their exact location. The measured instantaneous temperature of the perfect conductor is imposed on the boundary $x = x_b$ by taking trajectories from the perfect conductor (from Ω^*) and starting them in the boundary bin, with the prescription $x_0 = (\alpha \Delta t)^{1/2}$ as explained in case B.

Example:

Integration domain: [0, 1]

Boundary conditions: $-\partial T/\partial x = \partial T_{PC}/\partial t$ at $x = 0$ for $t > 0$

$\partial T/\partial x = 0$ at $x = 1$ for $t > 0$

Initial conditions: $T = 0$ for $0 \le x \le 1$; $T_{PC}(t = 0) = 1$

Analytical solution:

$$T^{an}(x, t) = \frac{1}{2} + 2 \sum_{k=1}^{\infty} \frac{e^{-q_k^2 t}}{2 + q_k^2} \frac{\cos[q_k(1-x)]}{\cos q_k}$$

where q_k is the kth solution of:

$$\tan q = -q \quad q > 0$$

In this example, we take the size, density, and specific heat of the perfect conductor to be the same as those of the integration domain. The agreement between the analytical and stochastic temperature profiles for four different times is shown in Figure 6.

Case F: boundary between two media: $K_1 \partial T_1/\partial x = K_2 \partial T_2/\partial x$

The physical meaning of this BC is equality of fluxes through an interface at x_b between two media with different thermal diffusivities. Since the equation to be solved is of the same form in both media, the identification with the FPE leads us to the same form of the SDE for both media, but the difference in thermal diffusivities implies that the term in the square root of Eqs. 5 and 6 will be different in the first and in the second medium. Without loss of generality we assume medium 1 to be the *low-mobility* medium: $\alpha_1 < \alpha_2$. The way to enforce the BC in the stochastic formulation is to perform the following operations at every integration step:

(i) Advance all currently active trajectories from (t_i, Y_i) to (t_{i+1}, Y_{i+1}) by Δt using Eq. 6 with $\alpha = \alpha_1$ if the trajectory is in medium 1 at t_i, $\alpha = \alpha_2$ if in medium 2.

(ii) Impose other boundary conditions.

(iii) For every trajectory, if both Y_i and Y_{i+1} are in the same medium, the step for that trajectory is completed.

(iv) For every trajectory, if Y_i is in the low-mobility medium ($Y_i < x_b$) and Y_{i+1} is in the high-mobility medium ($Y_{i+1} > x_b$), modify Y_{i+1} thus:

$$Y_{i+1}^{\text{mod}} = x_b + \frac{1}{r}\,(Y_{i+1} - x_b)$$

where $r = (\alpha_1/\alpha_2)^{1/2}$. The step for that trajectory is completed.

(v) For every trajectory, if Y_i is in the high-mobility medium ($Y_i > x_b$) and Y_{i+1} is in the low-mobility medium ($Y_{i+1} < x_b$), draw a random number R from a uniform distribution in [0, 1]. If $R < r$, modify Y_{i+1} thus:

$$Y_{i+1}^{\text{mod}} = x_b + r(Y_{i+1} - x_b)$$

otherwise, reflect Y_{i+1} at the boundary back into the high-mobility medium, as explained in case C for the reflecting boundary. The step for that trajectory is completed.

This algorithm acts on trajectories that cross the interface. Its effect is to modify the length of the portion of the step that lays in the medium into which the trajectory goes, shortening or lengthening it by a factor of r. Further, if a transition from the high-mobility medium into the low-mobility medium is attempted, this transition is rejected with probability $1-r$, in which case the trajectory is reflected at the boundary.

The modification of the length of the steps that cross the interface is necessary to ensure correct dynamic behavior in its neighborhood. It is simple to prove that $1/r$ is the factor to be used: let's consider the high mobility domain (medium 2) to have been contracted by a factor of $1/r$ and its thermal diffusivity to be the same as that of the low mobility medium (medium 1). The contracted domain 2 is denoted by 2^*. Trajectories performing a random walk in the transformed domain $1 \cup 2^*$ do not notice the presence of an interface, since the thermal diffusivities are the same, so their behavior across the interface is correct to all orders of Δt. The diffusive behavior is correct as well as 1 but wrong in 2^*, because the same α_1 is being used in both parts. If we now stretch 2^* and all parts of the trajectory embedded in it by the same factor $1/r$, so as to recover the original domain 2, the dynamics of the random walk will be correct across the interface and in *both* the low- and high-mobility media because the steps in medium 2^* will have been expanded by $1/r$. This is exactly what is achieved in steps iv and v. Although the proof of why some trajectories have to be reflected at the boundary is left for the Appendix, it is possible to gain an intuitive understanding if we consider that the trajectory density profile over $1 \cup 2^*$ has continuous derivative at the interface. After stretching 2^* back by $1/r$, the slope of the trajectory density profile shows a discontinuity at the interface: it is $1/r$ times lower in 2 than in 1. However, the boundary condition requires the slopes to differ by $1/r^2$, that is, the flux from the high-mobility into the low-mobility domain is too high by a factor of $1/r$. This factor is exactly compensated for in the first part of step v by rejecting transitions between 2 and 1 with probability $1-r$.

Example:

Integration domain: $[-1, 1]$

Boundary conditions: $\partial T_1/\partial x = 2\partial T_2/\partial x$ at $x=0$ for $t>0$

$\partial T_1/\partial x = 0$ at $x=-1$ for $t>0$

$\partial T_2/\partial x = 0$ at $x=+1$ for $t>0$

Initial conditions: $T=1$ for $-1 \le x \le 0$

$T=0$ for $0 \le x \le 1$

Analytical solution:

$$T_1^{\text{an}}(x, t) = \frac{1}{2} + 2\sum_{k=1}^{\infty} e^{-q_k^2 t}\,\frac{\sin q_k r \cos[q_k(1+x)]}{q_k[(r^2+1)\sin q_k \sin q_k r - 2r \cos q_k \cos q_k r]} \qquad x \le 0$$

$$T_2^{\text{an}}(x, t) = \frac{1}{2} - 2\sum_{k=1}^{\infty} e^{-q_k^2 t}\,\frac{r \sin q_k \cos[r q_k(1-x)]}{q_k[(r^2+1)\sin q_k \sin q_k r - 2r \cos q_k \cos q_k r]} \qquad x > 0$$

where q_k is the kth solution of:

$$r \tan q = -\tan rq \quad q > 0$$

In this example we have assumed $\alpha_1 = 1$, $\alpha_2 = 2$, all other physical properties to be equal to one and the two media to be of the same size. Since the total system formed by the two media is adiabatic, the integration domain Ω and the domain Ω^* coincide. At $t=0$, the whole ensemble of M trajectories is uniformly distributed throughout the left half of the interval $[-1, 1]$ ($T_1 = 1$, $T_2 = 0$). Figure 7 presents the comparison between analytical and stochastic solutions at four different times. In order to illustrate the effect of ensemble size, the curves for $t=0.01$ and $t=0.1$ were obtained with an ensemble of $M = 4 \times 10^6$ trajectories. The curves for $t=0.25$ and $t=0.5$ were obtained in a separate run with $M = 4 \times 10^4$ trajectories.

Case G: heat production

This case corresponds to the creation or anihilation of heat (or mass of a species) in the medium, due for example, to a chemical reaction. Strictly speaking, this is not another type of BC, but a different equation that contains a source term:

$$\frac{\partial T}{\partial t} = \alpha \frac{\partial^2 T}{\partial x^2} + \frac{S(t, x)}{\rho c}$$

In the stochastic approach the source term is realized by starting new trajectories at each time step throughout the integration domain according to the following prescription: let N_P be the (arbitrarily chosen) number of trajectories that we wish to assign to an energy production rate of 1 energy unit per unit time. Once this scale has been set, the total number of trajectories $N_{\text{Prod}}(t)$ to be started per integration step at time t is given by $N_{\text{Prod}}(t) = N_P \Delta t \int_\Omega S(t, z)dz$. The positions at which the $N_{\text{Prod}}(t)$ trajectories are started are given by a random variable x_0 whose distribution function is the normalized

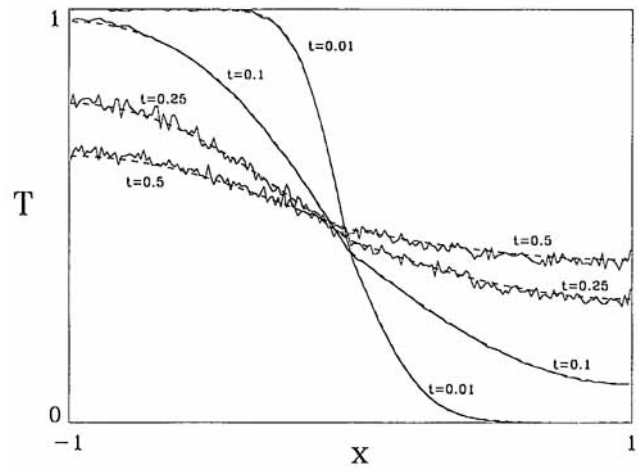

Figure 7. Boundary conditions f: boundary between two media of different physical properties.

Comparison of analytical (- - - -) and computed (—) temperature profiles at four different times. The thermal diffusivity in [0, 1] is twice as high as in [−1, 0]. $N_{bin} = 100$, $\Delta t = 10^{-5}$. To show the effect of ensemble size for the profiles at $t = 0.01$ and $t = 0.1$, a temperature of 1 corresponds to 4×10^4 trajectories per bin; the curves $t = 0.25$ and $t = 0.5$ were obtained in a different run for which a temperature of 1 corresponds to 4×10^2 trajectories per bin.

production term $\hat{S}(t, x) = S(t, x)/\int_\Omega S(t, z)dz$ (if S is not a function of x, x_0 is uniformly distributed in Ω). Values of x_0 are obtained by sampling $\hat{S}(t, x)$ by means of the rejection technique (Press et al., 1989) or any other suitable method. The temperature in a bin $[x, x + \Delta x]$ at a given time t is obtained by counting the number of trajectories that are present in that bin at t and multiplying this number by the normalization factor:

$$NF_{(g)} \equiv \frac{1}{N_P \Delta x \bar{\rho}(t, x)\bar{c}(t, x)}$$

Example:

Equation to be solved:

Integration domain: [0, 1]

$$\frac{\partial T}{\partial t} = \frac{\partial^2 T}{\partial x^2} + S(t, x)$$

Boundary conditions: $T = 0$ at $x = 0$ for $t > 0$

$T = 0$ at $x = 1$ for $t > 0$

Initial conditions: $T = 0$ for $0 \le x \le 1$

Heat source: Uniform per unit length of interval; intensity: $S(t, x) = e^{-t}$

Analytical solution:

$$T^{an}(x, t) = \left(\frac{\cos\left(\frac{1}{2} - x\right)}{\cos\frac{1}{2}} - 1 \right) e^{-t} - \frac{4}{\pi} \sum_{k=0}^{\infty} e^{-(2n+1)^2 \pi^2 t} \frac{\sin(2n+1)\pi x}{(2n+1)[(2n+1)^2\pi^2 - 1]}$$

In this example, heat production is uniform in space and exponentially decaying in time, so that the temperature profile rises to a maximum and then asymptotically returns to $T(t, x) = 0$. The spatially uniform source of heat is realized by starting new trajectories at each time step in the interval [0, 1] at random positions, these positions being chosen from a uniform distribution in [0, 1]. The number of new trajectories $N_{Prod}(t)$ to be created per time step varies with time proportionally to e^{-t}. The other two BCs correspond to absorbing boundaries like in case A above. Complete agreement between the analytical and the stochastic solution is obtained for $\Delta x = 0.01$ and $\Delta t = 10^{-5}$ (Figure 8a). Spatially dependent sources and point sources are treated analogously.

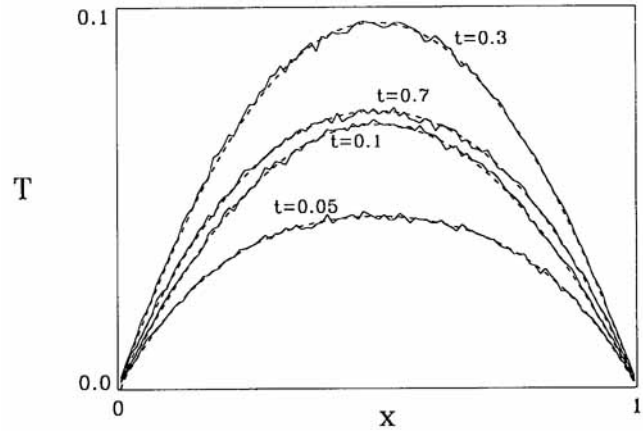

Figure 8a. Boundary conditions g: heat production.

Comparison of analytical (- - - -) and computed (—) temperature profiles at four different times. $N_{bin} = 100$, $\Delta t = 10^{-5}$, $N_P = 10^7$.

Up to now, the results shown in cases A through F were obtained with a relatively small integration step and the question of accuracy was not addressed. Although a discussion of convergence properties is not the main goal of the article, case G is ideally suited to study an important effect, namely that of the absorbing boundaries on the discretization error and on the order of convergence.

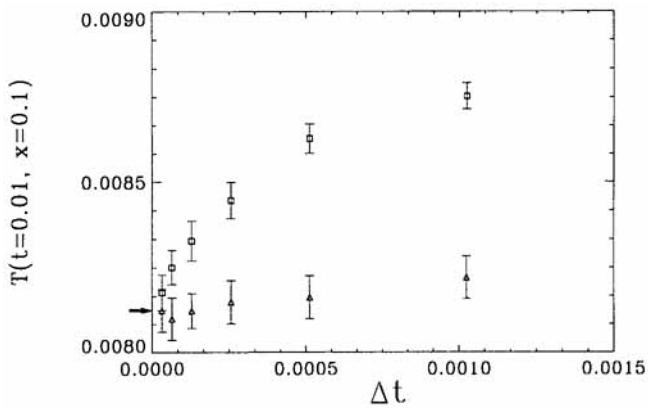

Figure 8b. Boundary conditions g: comparison of convergence order for the improved and the naive algorithms.

The arrow points to the exact solution $T_{an}(x = 0.1, t = 0.01)$, and the symbols correspond to the stochastic solution for different values of Δt. Naive algorithm, □; improved algorithm, △; one standard deviation of the average, 1. $N_{bin} = 20$, $N_P = 10^7$.

In Figure 8b we plot the stochastic solution at $t=0.01$ and $x=0.1$ (obtained with $\Delta x=1/20$ and $N_{\text{Prod}}/\Delta t=10^7$) as a function of Δt, as obtained by the straightforward algorithm described above (squares). The error bars represent the standard deviation of the mean obtained by performing 18 integrations for every value of Δt with 18 different seeds for the random number generator. The exact value of $T^{\text{an}}(t=0.01, x=0.1)$ is represented by the arrow on the ordinate axis. We see that as we reduce the step size, the stochastic solution does indeed converge to the exact value. Since the Euler-Maruyama method has a weak order of convergence of 1, we would expect the difference between the analytical and the stochastic solution to decrease linearly with Δt. However, the squares in Figure 8b show the clear signature of a square root dependence on Δt; a fit to powers of Δt indicates that the convergence is of order 0.52 ± 0.08. The source of this degraded order of convergence is the way the absorbing boundaries are treated. In contrast to deterministic ODEs, even if Y_i and $Y_{i+1}=Y_i+(2\alpha\Delta t)^{1/2}W_i$ for a given trajectory (Eq. 6) lie within [0, 1], there is a nonzero probability that the stochastic trajectory left the interval [0, 1] between t_i and t_{i+1}, especially when the trajectory is close to one of the boundaries. Such absorptions go unnoticed in an integration with discrete time and are known to be responsible for errors of order $(\Delta t)^{1/2}$ (Strittmatter, 1987; Öttinger, 1989). The proper way to eliminate the $(\Delta t)^{1/2}$ error is to compute the conditional probability for unobserved absorptions at the boundaries. This probability is given by (Strittmatter, 1987; Öttinger, 1989):

$$P=\exp\left[-\frac{1}{\alpha\Delta t}(B-Y_i)(B-Y_{i+1})\right]$$

where B is the coordinate of the appropriate boundary (either 0 or 1 in this example).

This probability is exponentially small and hence negligible except when the distance between the boundary B and Y_i is at most of order $(\Delta t)^{1/2}$. The obvious thing to do to remove the $(\Delta t)^{1/2}$ error is to terminate a trajectory with probability P even when no absorption at a boundary has been observed in the time interval $[t_i, t_{i+1}]$. The boundary B used to calculate P is 0 if $Y_{i+1}\le 0.5$ and 1 if $Y_{i+1}>0.5$. The results obtained with this improved algorithm are represented by the triangles in Figure 8b. Within error bars, the Euler-Maruyama method converges now with weak order 1 as it should (actually, with order 0.92 ± 0.18).

The improved algorithm not only recovers the order of convergence, but it allows us to use a larger integration step as well. The accuracy of the solution for $\Delta t=10^{-3}$ is now as good as it was for $\Delta t=10^{-5}$ with the naive algorithm. The improvement more than compensates for the additional computations needed to account for unobserved absorptions, which increase execution time by about 20%. The remaining error is of $O(\Delta t)$ and is due to the discretization of the heat production. The integration for several (not too small) values of Δt can be used to determine the order of convergence and to extrapolate to $\Delta t=0$ in order to obtain high accuracy solutions (Greiner et al., 1988; Öttinger, 1989) with moderate effort.

It is important to emphasize that unless unobserved absorptions are accounted for properly, the presence of absorbing boundaries (a typical example of so-called *first passage problems* (Strittmatter, 1987)) will in general lead to a reduction of the order of convergence. This feature is characteristic of SDEs and has no counterpart in deterministic differential equations.

Case H: moving boundary: $-k_1\partial T_1/\partial x+k_2\partial T_2/\partial x=L\rho dX_b(t)/dt$

In this case, the medium undergoes a first-order phase transition at T_m. At the boundary between both phases [located at $X_b(t)$] absorption of the latent heat L takes place. This heat is removed instantaneously from the heat-conduction process in which it takes no further part. The velocity of the phase coexistence boundary $dX_b(t)/dt$ is controlled by the rates at which heat is supplied and removed by conduction through the two phases. This is a nonlinear problem in the position of the boundary (Carslaw and Jaeger, 1959).

This BC, although involving derivatives, expresses that the phase transition boundary will move depending on the difference of the rates of heat arrival and removal due to conduction. In the stochastic dynamic method this is implemented as follows: let $X_b(t)$ be the position of the boundary at a given time t in the course of the integration and let's assume the boundary is moving towards growing x. At *every* integration step, perform the following operations:

(i) Advance all currently active trajectories by Δt using Eq. 6.

(ii) Enforce other boundary conditions (if present).

(iii) Monitor the temperature at X_b by determining the local density of trajectories, that is, by counting how many trajectories exist in the interval $[X_b(t)-0.5(\alpha\Delta t)^{1/2}, X_b(t)+0.5(\alpha\Delta t)^{1/2}]$ and converting to temperature as in case A. The temperature (density of trajectories) at X_b will have varied with respect to the previous step due to diffusion of trajectories *both* from $x<X_b(t)$ and from $x>X_b(t)$.

(iv) If the temperature (that is, the number of trajectories) measured at $X_b(t)$ is less than the phase transition temperature T_m, the step is completed. Return to (i).

(v) If the temperature measured at $X_b(t)$ is higher than the phase transition temperature T_m, the excess number of trajectories corresponds to latent heat to be removed. This is done by starting negative trajectories at $X_b(t)$ until the latent heat corresponding to an inverval of width $(\alpha\Delta t)^{1/2}$ has been removed or until the temperature at $X_b(t)$ has sunk back to T_m, whichever happens earlier. If N_L is the number of trajectories that we have assigned to one energy unit, every time a negative trajectory is started, the boundary advances by:

$$\frac{1}{N_L\bar{\rho}(t,x)\bar{c}(t,x)}$$

Step completed; return to (i).

The boundary between both phases acts thus as a moving point source that leaves behind a trail of negative trajectories. These subsequently diffuse throughout the whole domain. During the integration we will have positive or *hot* and negative or *cold* trajectories coexisting in the same simulation in the integration domain. Both types of trajectories follow the same dynamics and are integrated according to the same scheme (Eq. 6).

Case G is a combination of temperature monitoring, like in

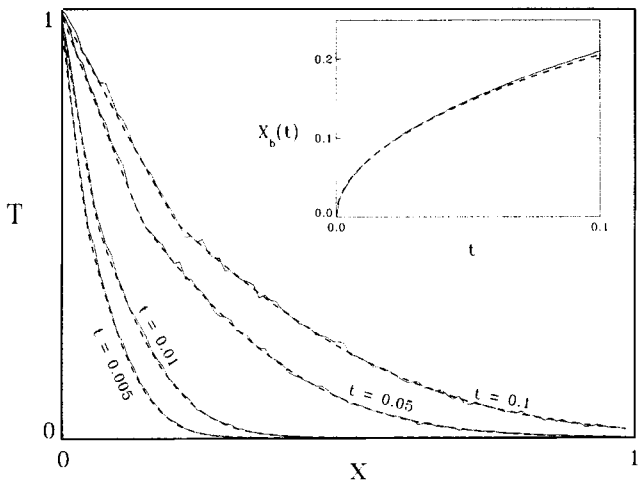

Figure 9. Boundary conditions h: moving boundary due to phase transition.

Comparison of analytical (- - - -) and computed (—) temperature profiles at four different times. $N_{bin} = 100$, $\Delta t = 10^{-5}$, $N_h = 2 \times 10^4$. The inset shows the position of the melting boundary X_b as a function of time.

the radiation boundary condition (case D), and enforcement of a time and position dependent sink (or source) term, both being done at a position $X_b(t)$ that has to be determined concurrently with the integration of the ensemble of trajectories.

Example:
Integration domain: $[0, +\infty]$
Boundary conditions: $T=1$ at $x=0$ for $t>0$
$-\partial T_1/\partial x + \partial T_2/\partial x = dX_b(t)/dt$,
where $X_b(t)$ is the position of the transformation boundary.
Initial conditions: $T=0$ for $0 \le x$
Analytical solution (for $T_m = 0.5$):
Position of the boundary:

$$X_b(t) = 2b\sqrt{t}$$

where b is the solution of

$$\frac{1}{\text{erf } b} - \frac{1}{\text{erfc } b} = 2\sqrt{\pi} b e^{b^2}$$

Temperature profile:

$$T^{an}(x, t) = \begin{cases} T_1^{an}(x, t) & \text{if } x \le X_b(t) \\ T_2^{an}(x, t) & \text{if } x > X_b(t) \end{cases}$$

$$T_1^{an}(x, t) = 1 - \frac{1}{2 \text{ erf } (b)} \text{ erf}\left(\frac{x}{2\sqrt{t}}\right)$$

$$T_2^{an}(x, t) = \frac{1}{2 \text{ erfc } (b)} \text{ erfc}\left(\frac{x}{2\sqrt{t}}\right)$$

In this example we deal with melting in a one-dimensional semi-infinite interval and we have assumed the melting temperature to be $T_m = 0.5$, the latent heat accompanying the phase change to be one and the other physical properties of both media to be the same and equal to unity. The change in volume accompanying melting has been neglected. The semi-infinite region is initially at $T=0$ and in contact with a heat source at $x_b = 0$ with constant temperature $T_b = 1$.

The BC $T_b = 1$ at $x_b = 0$ is of type case A. The moving boundary BC was treated according to the procedure explained above. Figure 9 presents the analytical and the stochastic solution at four different times. The temperature profiles are in perfect agreement. An even more stringent test of the quality of the solution is the determination of the position of the moving boundary. The inset compares the analytical (dashed line) and the stochastic solution. Besides the accuracy of the solution for $X_b(t)$, it is remarkable that the statistical noise in $X_b(t)$ is much lower than in the temperature profiles themselves. This could come out as a surprise, because the position of the moving boundary $X_b(t)$ depends not only on the derivative of a fluctuating temperature field, but actually on the difference of two such quantities, so that even stronger fluctuations could be expected. In the stochastic approach, however, the formulation of the BC corresponds more closely to the physical reality: the boundary moves due to removal of latent heat and not due to differences in the derivatives of the temperature field. Although trajectories arrive at the boundary X_b in a highly irregular way, the removal of the latent heat has in fact a cumulative or integral character that damps out the fluctuations in the fluxes. The stochastic dynamic approach naturally transforms a complex BC involving differences of derivatives into a simple physical process of integral character.

Further, the treatment of a semi-infinite domain ($x \ge 0$) is not problematic in the stochastic approach. Trajectories just continue to be integrated no matter how far to the right they may wander, but they may not be terminated because, due to the extreme variability of the paths of Wiener process, there is a nonzero chance that they will eventually return from any excursion in a region where x is large.

Computational Aspects

From the computational point of view, some key features of the stochastic dynamic approach are the following:

- The method does not require enmeshment of the integration domain. The division in bins is purely a measuring device and is not part of the calculation. Therefore, complex geometries can be dealt with easily. The only requirement is that it should be possible to decide whether a given sample path is within or without the integration domain.
- The computational effort grows with the size of the problem raised to the dimension of the integration domain, say N^3 in three dimensions, while in finite-difference or finite-elements methods it increases as N^6 or N^7. It is however unlikely that the stochastic dynamic approach can compete in terms of computational efficiency against a well-tuned deterministic equivalent, like, for example, multigrid-spectral approaches for diffusion problems.
- Obtaining high accuracy solutions with the stochastic approach is expensive, because of the $O(M^{1/2})$ convergence with sample size. However, for the same reason, low accuracy solutions can be obtained with very modest programming and

computational effort. Such solutions may be used as starting point for highly accurate discretization or spectral techniques.

- The stochastic method possesses desirable numerical stability properties. Besides, it is free from singularities arising from spatial or temporal discontinuities, as illustrated in cases A and C above.
- As indicated in case A, the stochastic dynamic approach yields, within the stochastic error due to finite sample size, the *exact* integral average value of the solution in a given bin (Eq. 7). In this sense, it is an exact method at the coarse-grained level defined by the bin size, no matter how coarse the binning is.
- The coding of a stochastic dynamic algorithm is very simple. The programs written to solve examples of cases A to H have fewer than 300 lines of FORTRAN code, including data preparation and output. The core routine that integrates the SDE is between 10 (case A) and 50 (case H) lines long.
- The stochastic dynamic approach is ideally suited to vector and parallel (or massively parallel) machines. Since the sample paths are essentially noninteracting, they can be processed in well-vectorizable loops and evenly distributed among any number of processors. The results presented above were computed on a scalar workstation (SGI). Additionally, vectorized code was developed on two supercomputers (a Cray Y-MP/464 and a NEC SX-3/22). A vectorized version of the algorithm A runs more than 40 times faster on the NEC SX-3 as the scalar version on an SGI Indigo. The vectorized version attains a sustained performance of about 70% peak on a Cray Y-MP processor.

Conclusions

We have introduced the stochastic dynamic (SD) approach to the solution of partial differential equations arising in transport phenomena. As a first step, we have presented the methodology for the case of linear PDEs, building on the analogy between Fokker-Planck equations and stochastic differential equations. The correct treatment of boundary conditions is decisive for the success and efficiency of the method. Using a simple one-dimensional example, we have shown that it is possible to deal with the eight basic types of boundary conditions (Crank, 1975).

The methodology described in this article is applicable to linear transport phenomena problems in any number of dimensions. It can also be applied to potential flow of incompressible fluids. However, in its present form the method is not adequate for general nonlinear transport phenomena. The reason for this is that the FP equation is a linear PDE. When dealing with nonlinear problems, the rigorous FP-SDE equivalence cannot be applied and other, more involved methods have to be used whose correct application requires care (van Kampen, 1981).

The SD method provides us with a physical interpretation of the processes underlying transport phenomena. Boundary conditions that are formulated mathematically as derivatives are more naturally implemented as fluxes in the SDE method. Singularities at temporal discontinuities that require special care in traditional discretization methods do not exist in the stochastic dynamic approach.

However, the great strength of the SD approach will be most apparent when the solution we are interested in is *not* the probability density function itself (that is, the temperature, concentration, or momentum fields) but some moment of that distribution. This is the case in the calculation of the stress tensor in polymer melts and solutions via stochastic dynamic simulation of model polymers. In such instances, the SD method can yield solutions to otherwise intractable problems (Öttinger, 1989, 1994).

Current work on the SD approach aims at the extension to higher dimensional problems, to coupled nonlinear problems and to general momentum transfer problems.

Acknowledgments

The author would like to thank H. C. Öttinger, U. W. Suter, J. J. de Pablo, M. Leontidis, M. Tomaselli, and W. Petersen for their very useful suggestions. The invaluable help of Michael Hodous at the Centro Svizzero di Calcolo Scientifico (CSCS) with program vectorization is greatly appreciated. Generous allocations of CPU-time on the Cray Y-MP/464 of the Swiss Federal Institute of Technology and on the NEC SX-3 of the CSCS in Manno are gratefully acknowledged.

Notation

a = transmission factor
$A(t, x)$ = drift vector
c = specific heat
c_{PC} = specific heat of the perfect conductor
$D(t, x)$ = diffusion matrix
$E(\ )$ = expectation value
F_b = flux at the boundary
h = heat-transfer coefficient
k = thermal conductivity
L = latent heat
M = ensemble size; number of trajectories
$N(0, 1)$ = Gaussian distribution of mean 0 and variance 1
$NF_{(a)}, \ldots$ = normalization factor for case A
N_{bin} = number of bins
N_{Flux} = number of trajectories that correspond to a flux F_b
N_P = number of trajectories that correspond to production of 1 energy unit per unit time
N_{PC} = number of trajectories in perfect conductor
$N_{\text{Prod}}(t)$ = number of trajectories corresponding to heat production
N_{step} = number of integration steps
N_1 = number of trajectories per bin corresponding to $T = 1$
$p(t, x)$ = probability density
$P(\ )$ = probability
r = square root of the ratio of thermal diffusivities in two media
R = random number from uniform distribution in [0, 1]
$S(t, x)$ = source term
$\hat{S}(t, x)$ = normalized source term
t = time
Δt = time integration step
T = temperature
T_b = temperature at a boundary
T_0 = temperature of the surrounding medium
T_{PC} = temperature of the perfect conductor
T_S = temperature at the surface
V_{PC} = volume of the perfect conductor
W = Wiener process
x = coordinate
x_b = position of fixed boundary
$X_b(t)$ = position of the moving boundary
Δx = width of measuring bin
Δx_b = width of boundary region
Y = time discrete approximation
z = dummy integration variable

Greek letters

α = thermal diffusivity
β = order of convergence

ϵ = average integration error
ρ = density
ρ_{PC} = density of the perfect conductor
Ω = integration domain
Ω^* = "limbo" domain

Literature Cited

Allen, M. P., and D. J. Tildesley, *Computer Simulation of Liquids*, Clarendon Press (1987).

Bird, R. B., R. C. Armstrong, and O. Hassager, *Dynamics of Polymeric Liquids: I. Fluid Mechanics*, Wiley, New York (1987a).

Bird, R. B., C. F. Curtiss, R. C. Armstrong, and O. Hassager, *Dynamics of Polymeric Liquids: II. Kinetic Theory*, Wiley, New York (1987b).

Bird, R. B., W. E. Stewart, and E. N. Lightfoot, *Transport Phenomena*, Wiley, New York (1960).

Carslaw, H. S., and J. C. Jaeger, *Conduction of Heat in Solids*, 2nd ed., Oxford University Press (1959).

Chawla, T. C., ed., *Annual Review of Numerical Fluid Mechanics and Heat Transfer*, Hemisphere (1989).

Crank, J., *The Mathematics of Diffusion*, 2nd ed., Oxford University Press (1975).

Ermak, D. L., and G. A. McCammon, "Brownian Dynamics with Hydrodynamic Interactions," *J. Chem. Phys.*, **69**(4), 1352 (1978).

Fixman, M., "Implicit Algorithm for Brownian Dynamics of Polymers," *Macromolec.*, **19**, 1195 (1986).

Gard, T. C., *Introduction to Stochastic Differential Equations*, Marcel Dekker (1988).

Gardiner, C. W., *Handbook of Stochastic Methods for Physics, Chemistry and the Natural Sciences*, Springer Verlag (1983).

Greiner, A., W. Strittmatter, and J. Honerkamp, "Numerical Integration of Stochastic Differential Equations," *J. Stat. Phys.*, **51**(1/2), 95 (1988).

Hirata, M., and N. Kasagi, eds., *Transport Phenomena in Turbulent Flows: Theory, Experiment, and Numerical Simulation*, Hemisphere (1988).

Honerkamp, J., *Stochastische Dynamische Systeme*, VCH, Weinheim (1990).

Ikeda, N., and S. Watanabe, *Stochastic Differential Equations and Diffusion Processes*, 2nd ed., North Holland (1989).

Itô, K., "Differential Equations Determining Markov Processes," *Zenkoku Shijo Sugaku Danwakai*, **244**(1077), 1352 (1942).

Kalos, M. H., and P. A. Whitlock, *Monte Carlo Methods*, Wiley (1986).

Kallianpur, G., *Stochastic Filtering Theory*, Springer Verlag (1980).

van Kampen, N. G., *Stochastic Processes in Physics and Chemistry*, North Holland (1981).

Kloeden, P. E., and E. Platen, *Numerical Solution of Stochastic Differential Equations*, Springer Verlag (1992).

Landau, L. D., and E. M. Lifshitz, *Fluid Mechanics*, 2nd English ed., Pergamon Press (1987).

Markatos, N., ed., *Numerical Simulation of Fluid Flow and Heat/Mass Transfer Processes*, Springer Verlag (1986).

Maruyama, G., "Continuous Markov Processes and Stochastic Equations," *Rend. Circolo Math. Palermo*, **4**, 48 (1955).

Öttinger, H. C., "Computer Simulation of Reptation Theories: I. Doi-Edwards and Curtiss-Bird Models," *J. Chem. Phys.*, **91**(10), 6455 (1989).

Öttinger, H. C., "Computer Simulation of Reptation Theories: II. Reptating-Rope Model," *J. Chem. Phys.*, **92**(7), 4540 (1990).

Öttinger, H. C., *Stochastic Processes in Polymeric Fluids*, Springer Verlag, in preparation (1994).

Patankar, S. V., *Numerical Heat Transfer and Fluid Flow*, McGraw-Hill, New York (1980).

Petersen, W. P., "Some Experiments on Numerical Simulations of Stochastic Differential Equations and a New Algorithm," IPS Research Report No. 92-05, ETH Zürich (1992).

Press, W. H., B. P. Flannery, S. A. Teukolsky, and W. T. Vetterling, *Numerical Recipes; The Art of Scientific Computing*, Cambridge University Press (1989).

Risken, H., *The Fokker-Planck Equation*, Springer Verlag (1989).

Strittmatter, W., "Numerical Simulation of the First Passage Time," preprint, Univ. Freiburg, THEP 87/12 (1987).

Appendix

Assume the boundary between the two media to be at $x_b = 0$, medium 1 to be the interval $[-\infty, 0]$ and medium 2 to be $[0, +\infty]$. Let $p_1(x)$ be the probability density in medium 1 and $p_2(x)$ in medium 2. Trajectories can perform the transition $1 \rightarrow 2$ unimpeded. For the transition $2 \rightarrow 1$, trajectories are reflected back into 2 with probability $1 - a$ (transmission factor a). The flux from $1 \rightarrow 2$ across the interface is given by:

$$\frac{1}{\Delta t}\int_0^\infty p_1(-x)P[\sqrt{2\alpha_1\Delta t}N(0,1)>x]dx$$

$$=\frac{1}{\Delta t}\int_0^\infty p_1(-x)P\left[N(0,1)>\frac{x}{\sqrt{2\alpha_1\Delta t}}\right]dx$$

$$=\frac{1}{\Delta t}\int_0^\infty p_1(-x)\left(1-\text{erf}\,\frac{x}{\sqrt{\alpha_1\Delta t}}\right)dx$$

expanding p_1 to first order at the interface,

$$\frac{1}{\Delta t}\int_0^\infty [p_1(0)-xp_1'(0)]\left(1-\text{erf}\,\frac{x}{\sqrt{\alpha_1\Delta t}}\right)dx$$

$$=p_1(0)\sqrt{\frac{\alpha_1}{\pi\Delta t}}-\frac{1}{4}p_1'(0)\alpha_1$$

for the second medium we arrive in the same way at:

$$\frac{a}{\Delta t}\int_0^\infty [p_2(0)+xp_2'(0)]\left(1-\text{erf}\,\frac{x}{\sqrt{\alpha_2\Delta t}}\right)dx$$

$$=a\left[p_2(0)\sqrt{\frac{\alpha_2}{\pi\Delta t}}+\frac{1}{4}p_2'(0)\alpha_2\right]$$

so that the net flux across the interface is:

$$\frac{p_1(0)\sqrt{\alpha_1}-ap_2(0)\sqrt{\alpha_2}}{\sqrt{\pi\Delta t}}$$

$$-\frac{1}{2}\frac{p_1'(0)\alpha_1+ap_2'(0)\alpha_2}{2}+O(\sqrt{\Delta t}) \quad \text{(A1)}$$

Since the flux has to remain bounded for $\Delta t \rightarrow \infty$, the numerator of the first term has to vanish. Therefore,

$$a=\frac{p_1(0)}{p_2(0)}\sqrt{\frac{\alpha_1}{\alpha_2}} \quad \text{(A2)}$$

Since we require the temperature (probability density) to be continuous at the interface, $p_1(0) = p_2(0)$, a must be

$$a=\sqrt{\frac{\alpha_1}{\alpha_2}}$$

that is, the r defined in boundary condition f.

In mass-transfer problems, it is usual to have discontinuous concentration across the interface, fulfilling some (possibly

linear) relationship $p_2(t, x_b) = f[p_1(t, x_b)]$. The corresponding transmission factor is obtained by substituting the latter expression in Eq. A2. In such cases, a is not constant, but a function of the instantaneous values of the concentrations at the interface. It is remarkable that the condition of vanishing numerator of the first term of Eq. A1 has exactly the meaning of a detailed balance (Kalos and Whitlock, 1986). In this context, however, the detailed balance condition is truly dynamic, instead of representing a static balance, as usually encountered in Monte Carlo simulation techniques (Allen and Tildesley, 1987).

Manuscript received Apr. 19, 1993, and revision received Aug. 16, 1993.